A Cross-Shaped Dielectric Resonator Antenna for Multifunction and Polarization Diversity Applications

Longfang Zou, *Student Member, IEEE*, and Christophe Fumeaux, *Senior Member, IEEE*

***Abstract*—This letter proposes a multifunction cross-shaped dielectric resonator antenna (DRA) with separately fed broadside circularly polarized (CP) and omnidirectional linearly polarized (LP) radiation patterns. These distinct radiation patterns are achieved in overlapping frequency bands by exciting two different modes in a single dielectric resonator (DR) volume. This letter also investigates the effect of the feeding geometry on the mutual coupling between the modes and concludes that an asymmetric feeding degrades the orthogonality of the modes and thus increases the interport coupling coefficient. By using a symmetric feeding, the coupling coefficient can be significantly reduced to below −30 dB in the frequency band common to both operation modes. The experimental results show a good agreement with simulation and demonstrate a broadside CP operation over a bandwidth of 6.8%, which overlaps with the omnidirectional LP impedance bandwidth of 38.5%. The proposed antenna could be used not only as multifunction, but also as polarization diversity antenna due to the overlapping dual-feed CP and LP operation.**

***Index Terms*—Coupling coefficient, dielectric resonator antenna (DRA), multifunction, polarization diversity.**

I. Introduction

The PREVALENCE of wireless communication puts high demand on performance characteristics of highly integrated mobile wireless communication devices with versatile applications. Commonly, two or more antennas have to be employed in conventional multifunction or diversity schemes. It is a challenge to integrate such antennas into equipment taking space limitation, port-to-port isolation, or mutual effects of other elements into account.

Using a single-antenna structure with low mutual power coupling between different ports is one of the solutions to enable multifunction or diversity schemes. The available literature mostly focuses on multiports printed diversity antenna or planar inverted-F antenna (PIFA) due to their compactness, low cost, and low profile [1]–[4]. However, these antennas often have complicated structure, large size, or relatively low gain. Compared to conventional conductor-based antennas, dielectric resonator antennas (DRAs) have attractive features such as small size, high radiation efficiency, and versatility in their shape and feeding mechanism [5], [6]. Importantly, various modes with diverse radiation characteristics can be excited within a single DRA element. These modes can be utilized for various requirements, which makes the DRA a suitable potential candidate for multifunction applications. For example, a rectangular hollow dielectric resonator (DR) was designed as antenna and packaging cover [7]; ultrawideband operation was achieved by exciting the fundamental and higher-order modes in a hybrid DRA [8]; a cylindrical DRA was utilized as direction finder [9]; a cylindrical DR was used as filter and antenna [10]; a dual-band antenna with two different radiation patterns in two separate bands was achieved by using a cylindrical DR [11].

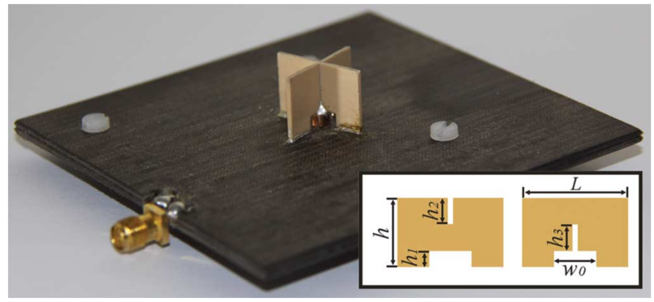

Fig. 1. Realized prototype of cross-shaped DRA. Inset: Notched rectangular dielectric plates forming the cross-shaped DR.

In this letter, we present a DRA with broadside circularly polarized (CP) and vertically polarized omnidirectional radiation patterns obtained by exciting two different modes within a cross-shaped DR. Compared to [11], the operation of two ports feeding a single-antenna volume with different radiation characteristics is achieved at the same frequency, which results in a multifunction, but also allows diversity. The size of the DR is reduced by using thin plates of high-permittivity material, as successfully applied in dual-mode bridge-shaped DRAs [12] and circularly polarized DRA [13]. In addition, a feeding with sequential rotation technique is utilized to increase the symmetry of the modes and reduce coupling between the two feeding ports.

II. Antenna Design

The proposed antenna is illustrated in Fig. 1. A cross-shaped DR is mounted on a Rogers substrate with backside metallization. The square substrate has a dielectric permittivity of 2.5, side length of 90 mm, and thickness of 1.524 mm. The cross-shaped DR is composed of two notched rectangular slices cut from the dielectric plate with thickness $d_0 = 1$ mm and permittivity of $\varepsilon_r = 50$. In each slice, a narrow notch with a width equal to the plate width d_0 is cut, as shown in the inset of Fig. 1,

Manuscript received April 20, 2011; revised June 21, 2011; accepted July 13, 2011. Date of publication July 22, 2011; date of current version August 01, 2011. The work of C. Fumeaux was supported by the Australian Research Council (ARC) Future Fellowship funding scheme (Project no. FT100100585).

The authors are with the School of Electrical and Electronic Engineering, The University of Adelaide, Adelaide, SA 5005, Australia (e-mail: lfzou@eleceng.adelaide.edu.au; cfumeaux@eleceng.adelaide.edu.au).

Color versions of one or more of the figures in this letter are available online at http://ieeexplore.ieee.org.

Digital Object Identifier 10.1109/LAWP.2011.2162479

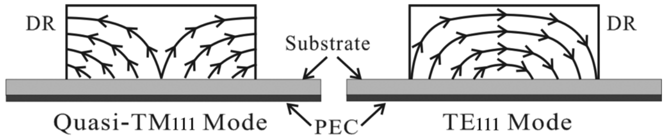

Fig. 2. Quasi-TM_{111} and TE_{111} mode in one arm of the cross-shaped DR.

TABLE I
ANTENNA PARAMETERS

Symbol	Value (mm)	Symbol	Value (mm)	Symbol	Value (mm)
L	20	h	13	h_1	3
h_2	5	h_3	5	w_0	8
d_0	1	L_0	6	L_1	7
d_1	1	L_2	16	d_2	1
L_3	25	d_3	1	L_4	21
d_4	1	L_5	11.2	d_5	2
d_6	4.35	w	0.5		

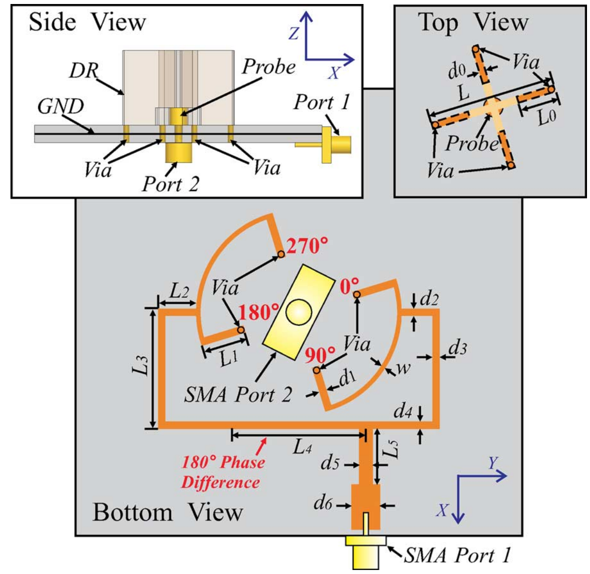

Fig. 3. Top, side, and bottom view of proposed antenna.

to create a mechanically stable cross. The wider notch with width w_0 provides room for a central probe feed. The detailed design procedures of a similar DR for a 4.5-GHz CP antenna can be found in [13]. For the sake of convenience, the dimensions of the resonator arms, including the notch, are listed in the first three lines of Table I.

The multiple functions of the antenna are realized by introducing two ports exciting independent orthogonal modes in the DR volume. The linearly polarized omnidirectional radiation pattern is realized by exciting a monopole mode, denoted here as Quasi-TM_{111} in reference to the corresponding cylindrical resonator mode. Circular polarization is achieved by exciting orthogonal TE_{111} modes in the two cross arms with 90° phase difference. The corresponding field distributions in one arm are sketched in Fig. 2. Hence, the design of the feeding networks is divided into three steps: 1) exciting Quasi-TM_{111} mode from port 2; 2) exciting quadrature TE_{111} modes from port 1; and 3) integrating these two ports into a common volume. The DRA element and feeding network are simulated and optimized by using Ansoft HFSS employing the finite-element method (FEM) in the frequency domain.

The Quasi-TM_{111} mode is excited through the widened center probe (diameter 3 mm) of an SMA connector located in the center of the cross, as shown in Fig. 3. As mentioned before, the bottom of the dielectric cross is cut to provide room for this center probe. The length and height of the notch are optimized for better coupling from the probe to the DR. Due to the high permittivity of the DR, the probe has to touch the DR to achieve efficient excitation of the Quasi-TM_{111} mode. For the same reason, the diameter of the probe (above the substrate part) is increased to improve coupling between the probe and DR in the simulation. This allows also to shorten the probe and increase the impedance bandwidth. In the antenna prototype, copper tape is wrapped around the probe to attain the optimal radius.

An initial feeding network design for the excitation of the TE_{111} mode is derived from the concept proposed in [13]. In that paper, orthogonal TE_{111} modes were excited in quadrature in the two equal-length dielectric cross arms. This was realized through microstrip lines with a 90° delay line. This feeding network introduces, however, an asymmetry in the geometry that degrades the symmetry of the TEM_{111} modes. This translates into asymmetric radiation patterns and reduces the usable angle around broadside where circular polarization is maintained to less than 30°.

To overcome these negative effects, a physical separation is first introduced in the form of a ground plane between the DR and its feeding network, as shown in Fig. 3. On the top substrate, the last segments of the feeding microstrip lines are under the DR cross. Their length is optimized for best impedance matching. The T-junction and delay line are located on the bottom of the lower substrate to reduce their impact on the radiation pattern. Vias are utilized to connect the T-junction to the feeding microstrip lines through holes in the ground plane and substrates.

The coupling between pure Quasi-TM_{111} and TE_{111} modes is theoretically zero due to the orthogonal field distribution of these two modes. Using two feeding points of the cross for CP operation as in [13], the simulation results indicate that the coupling between the CP and LP ports will be more than -10 dB, which is not acceptable for a diversity antenna. This high coupling results from the asymmetrical feeding, i.e., with a feeding point at only one end of each cross arm. This introduces an asymmetry in the TE_{111} mode distribution in the DR volume, which destroys the ideal orthogonality of the Quasi-TM_{111} and TE_{111} modes. A sequential rotation technique, which is a commonly used feeding method in array [14], is preferred to achieve a symmetrical feeding. The feed network is modified so that DRA are fed by four feeding points with progressive 90° phase shift. The phase distribution is achieved with properly designed delay lines, as shown in Fig. 3. All dimensions of the antenna are listed in Table I. The simulation and measurement results demonstrate a significant reduction of coupling, as shown in Section III.

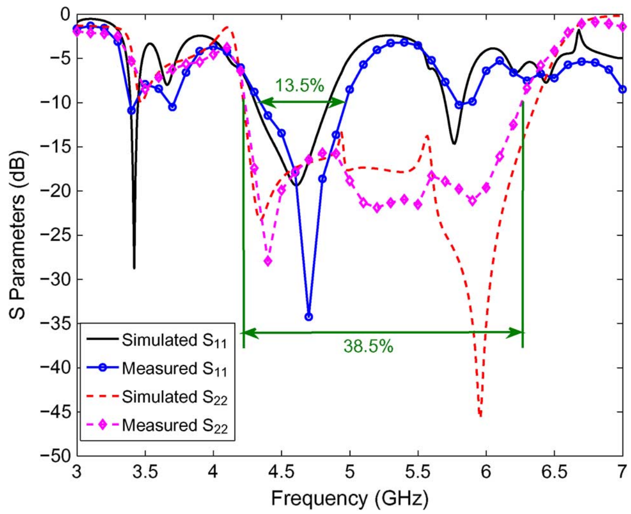

Fig. 4. Simulated and measured antenna reflection coefficient for port 1 (TE_{111} mode) and port 2 (Quasi-TM_{111} mode).

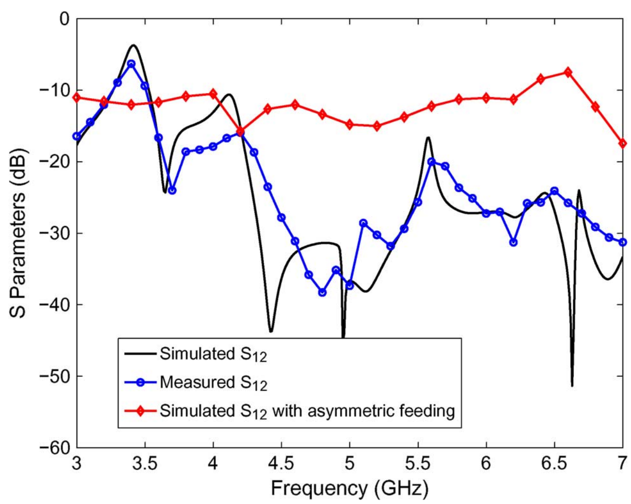

Fig. 5. Simulated and measured coupling coefficient between the two ports of the antenna. The asymmetric CP feed is simulated as in [13].

III. Antenna Performance

The simulated and measured reflection coefficients for the dual-feed antenna are shown in Fig. 4. The port 1 excites the TE_{111} modes and presents an impedance bandwidth (defined for $S_{11} < -10$ dB) of 13.5%, whereas the port 2 excites the Quasi-TM_{111} mode with a 38.5% impedance bandwidth. A small offset between simulated and measured reflection coefficient is attributed to fabrication imperfections.

Fig. 5 demonstrates a significant reduction of coupling between these two modes as a result of using a sequential symmetrical feeding. The simulated and measured results validate the concept that an asymmetric feeding (as in [13]) can disturb the symmetric mode distribution and hence increase coupling coefficient between different modes in the DR volume. The coupling coefficient can be reduced by using symmetric feeding. With the symmetric feeding, the coupling coefficient is below -15 dB in both CP and LP bandwith.

The axial ratio of the circular polarized mode (Port 1) is measured and calculated according to the third definition of

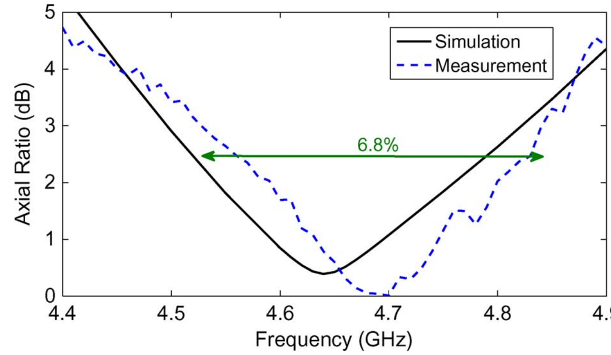

Fig. 6. Simulated and measured axial ratio for port 1.

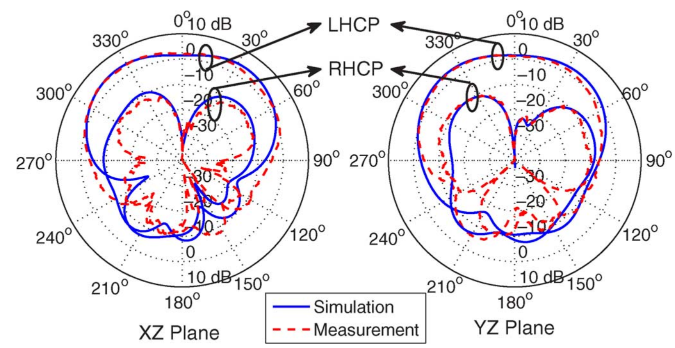

Fig. 7. Simulated and measured CP radiation pattern (port 1) at 4.69 GHz.

Ludwig [15]. Fig. 6 shows a comparison between simulated and measured axial ratio in broadside direction ($\theta = 0^{\circ}$). The 3-dB axial-ratio bandwidth extends from 4.52 to 4.84 GHz and yields an overlap with the impedance bandwidth of 6.8%. The frequency shift by 0.06 GHz to higher frequency is again attributed to fabrication imperfection. Over the CP bandwidth, the coupling coefficient between the two ports (Fig. 5) is below -30 dB. It is worth mentioning that the impedance and CP bandwidth might possibly be further increased by using an hybrid-ring feeding network or operating the antenna in a sequentially fed 2×2 subarray [14], [16] for high-gain applications.

The circular and linear polarization radiation patterns have been measured in the respective bands of the two ports. Sample patterns are shown here for 4.69 GHz, i.e., in the center of the overlapping frequency band. For port 1, broadside patterns with left-hand CP (LHCP) radiation patterns are obtained in both xz and yz planes, as shown in Fig. 7. The LHCP fields are at least 20 dB higher than right-hand CP (RHCP) fields in the broadside direction. The angle off broadside, where CP is achieved, extends to more than 60° with reasonably rotationally symmetric radiation pattern. The Ommnidirectional Quasi-TM_{111} radiating mode yields a vertically polarized monopole-type radiation patterns, as shown in Fig. 8. The simulated and measured cross-polarization levels are at least 20 dB lower than copolarization levels. In their operation bandwidths, the maximum gain of circularly and linearly polarized patterns are in the range of 4.5–5.5 and 2–4 dB, respectively.

The proposed antenna could also be used as a diversity antenna due to the wide bandwidth overlap of the omnidirectional LP and broadside CP patterns. Two commonly used

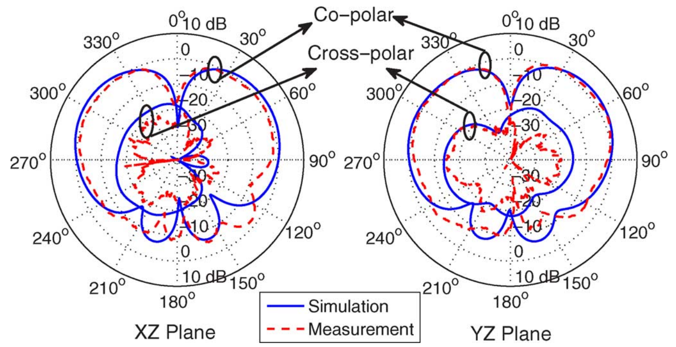

Fig. 8. Simulated and measured LP radiation pattern (port 2) at 4.69 GHz.

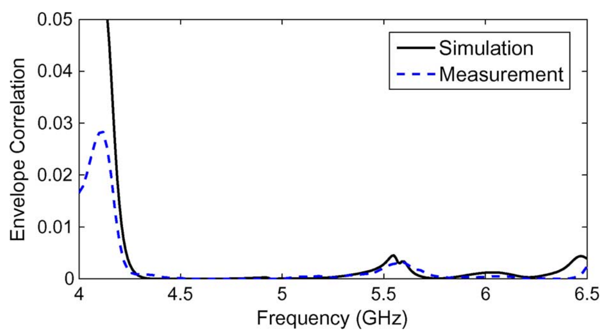

Fig. 9. Simulated and measured envelope correlation coefficients.

criteria—i.e., the envelope correlation [17] and the mean effective gain (MEG) [18]—are utilized to evaluate the antenna diversity performance. The envelope correlation coefficient for N-port antenna can be expressed in terms of S-parameters and a criteria $\rho_e < 0.5$ is commonly regarded as acceptable. The envelope correlation coefficients for the simulated and measured S-parameters as shown in Fig. 9 demonstrate the low correlation coefficients between the two ports. Additionally, for multiport antennas, all ports need to have a MEG that is approximately equal and as high as possible. The MEG will be -3 dB for 100% radiation efficiency, and it should be above -10 dB. The simulated and measured results show the MEG of ports 1 and 2 are both between -3.1 and -3.5 dB in the overlapping bandwidth. The MEG difference between ports 1 and 2 is less than 0.15 dB.

IV. Conclusion

This letter proposed a cross-shaped DRA for multifunction or diversity applications. A broadside CP and an omnidirectional LP patterns are radiated in overlapping frequency bands by exciting TE_{111} and Quasi-TM_{111} modes in a single cross-shaped DR, respectively. The mutual coupling between the excited resonator modes has been significantly reduced by using a symmetrical feeding network based on sequential rotation technique. Both simulated and measured results demonstrate good diversity antenna performance in terms of port isolation, envelope correlation coefficient, and mean effective gain.

References

[1] S.-L. Yang, K.-M. Luk, H.-W. Lai, A.-A. Kishk, and K.-F. Lee, "A dual-polarized antenna with pattern diversity," *IEEE Antennas Propag. Mag.*, vol. 50, no. 6, pp. 71–79, Dec. 2008.
[2] V. Plicanic, B. K. Lau, A. Derneryd, and Z. Ying, "Actual diversity performance of a multiband diversity antenna with hand and head effects," *IEEE Trans. Antennas Propag.*, vol. 57, no. 5, pp. 1547–1556, May 2009.
[3] A. Chebihi, C. Luxey, A. Diallo, P. Le Thuc, and R. Staraj, "A novel isolation technique for closely spaced PIFAs for UMTS mobile phones," *IEEE Antennas Wireless Propag. Lett.*, vol. 7, pp. 665–668, 2008.
[4] A. Diallo, C. Luxey, P. Le Thuc, R. Staraj, and G. Kossiavas, "Study and reduction of the mutual coupling between two mobile phone PIFAs operating in the DCS1800 and UMTS bands," *IEEE Trans. Antennas Propag.*, vol. 54, no. 11, pp. 3063–3074, Nov. 2006.
[5] A. Petosa and A. Ittipiboon, "Dielectric resonator antennas: A historical review and the current state of the art," *IEEE Antennas Propag. Mag.*, vol. 52, no. 5, pp. 91–116, Oct. 2010.
[6] K. M. Luk and K. W. Leung*, Dielectric Resonator Antennas*. Baldock, England: Research Studies, 2003.
[7] E. H. Lim and K. W. Leung, "Novel application of the hollow dielectric resonator antenna as a packaging cover," *IEEE Trans. Antennas Propag.*, vol. 54, no. 2, pp. 484–487, Feb. 2006.
[8] M. N. Jazi and T. A. Denidni, "Design and implementation of an ultrawideband hybrid skirt monopole dielectric resonator antenna," *IEEE Antennas Wireless Propag. Lett.*, vol. 7, pp. 493–496, 2008.
[9] L. Hady, A. Kishk, and D. Kajfez, "Dielectric resonator antenna utilization as a direction finder," in *Proc. IEEE APSURSI*, Jun. 2009, pp. 1–4.
[10] E. H. Lim and K. W. Leung, "Use of the dielectric resonator antenna as a filter element," *IEEE Trans. Antennas Propag.*, vol. 56, no. 1, pp. 5–10, Jan. 2008.
[11] L. K. Hady, A. A. Kishk, and D. Kajfez, "Dual-band compact DRA with circular and monopole-like linear polarizations as a concept for GPS and WLAN applications," *IEEE Trans. Antennas Propag.*, vol. 57, no. 9, pp. 2591–2598, Sep. 2009.
[12] G. Almpanis, C. Fumeaux, and R. Vahldieck, "Dual-mode bridge-shaped dielectric resonator antennas," *IEEE Antennas Wireless Propag. Lett.*, vol. 9, pp. 103–106, 2010.
[13] L. Zou and C. Fumeaux, "High-permittivity cross-shaped dielectric resonator antenna for circular polarization," in *Proc. Int. Conf. Electromagn. Adv. App.*, Sep. 2010, pp. 1–4.
[14] A. Petosa, A. Ittipiboon, and M. Cuhaci, "Array of circular-polarised cross dielectric resonator antennas," *Electron. Lett.*, vol. 32, no. 19, pp. 1742–1743, Sep. 1996.
[15] A. Ludwig, "The definition of cross polarization," *IEEE Trans. Antennas Propag.*, vol. AP-21, no. 1, pp. 116–119, Jan. 1973.
[16] S. Yang, R. Chair, A. A. Kishk, K. F. Lee, and K. M. Luk, "Circular polarized elliptical dielectric resonator antenna sub array fed by hybrid-ring feeding network," in *Proc. IEEE Int. Symp. Antennas Propag.*, Jul. 2006, pp. 2221–2224.
[17] S. Blanch, J. Romeu, and I. Corbella, "Exact representation of antenna system diversity performance from input parameter description," *Electron. Lett.*, vol. 39, no. 9, pp. 705–707, May 2003.
[18] T. Taga, "Analysis for mean effective gain of mobile antennas in land mobile radio environments," *IEEE Trans. Veh. Technol.*, vol. 39, no. 2, pp. 117–131, May 1990.